

Variety of chemical compositions of the clinopyroxenes from the eclogites (Seba eclogitic basic schists) in the Sambagawa metamorphic belt, central Shikoku, Japan

Md. Fazle KABIR and Akira TAKASU

Department of Geoscience, Faculty of Science and Engineering, Shimane University,

1060 Nishikawatsu, Matsue 690-8504, Japan

M. F. KABIR: fazlekabir@gmail.com

A. TAKASU: takasu@riko.shimane-u.ac.jp

Abstract

Seba eclogitic basic schists consist of garnet, clinopyroxene, amphibole, epidote and phengite, minor amounts of rutile, titanite, albite, paragonite, chlorite, hematite and quartz. Clinopyroxenes in the Seba eclogitic basic schists represent a variety of modes of occurrence (Cpx 1–5) and a wide range of the chemical compositions such as omphacite, aegirine-augite and augite. Aegirine-augite and omphacite (Cpx-1, $X_{Jd} = 0.23–0.39$ and $X_{Aeg} = 0–0.29$) occur as inclusions in porphyroblastic garnets. Omphacite (Cpx-2, $X_{Jd} = 0.29–0.37$ and $X_{Aeg} = 0.08–0.15$) occur as inclusions in the large-grained epidotes. Omphacite (Cpx-3) occurring as a schistosity forming mineral is clinopyroxene with highest jadeite contents ($X_{Jd} = 0.24–0.48$ and $X_{Aeg} = 0–0.25$). Omphacite (Cpx-4, $X_{Jd} = 0.25–0.36$ and $X_{Aeg} = 0.10–0.24$) is randomly oriented to the matrix schistosity. Omphacites are partly replaced by symplectites of clinopyroxene (Cpx-5) with lesser jadeite content (augite and aegirine-augite, $X_{Jd} = 0.10–0.19$ and $X_{Aeg} = 0.01–0.36$) with sodic-calcic/calcic-amphiboles (e.g. barroisite, edenite, Mg-hornblende, actinolite) and albite ($An < 4$). Cpx-1 and Cpx-2 are formed during the prograde epidote–amphibolite to the peak eclogite facies stages. The peak eclogite facies stage is represented by the occurrences of Cpx-3 and Cpx-4. Cpx-5 represented retrograde stage is defined by the phases replacing the minerals of the peak metamorphic stage.

Key words: Sambagawa (Sanbagawa) metamorphic belt, clinopyroxene, Sebadani, Besshi district.

1. Introduction

The Sambagawa metamorphic belt is a Cretaceous high P/T -type metamorphic belt in Japan, and it extends from the Kanto Mountains, through Kii Peninsula and Shikoku to Kyushu for over 800 km with maximum width of 50 km in Shikoku (Fig. 1). The protoliths are dominated by sandstone and shale with a small amount of basalt, chert and limestone. Metamorphic grade ranges from prehnite–pumpellyite facies through blueschist/greenschist facies to amphibolite facies and locally to eclogite facies (e.g. Banno, 1964; Higashino, 1990; Enami *et al.*, 1994). In the Besshi district the metamorphic belt is divided into four zones based on index minerals in pelitic schists (e.g. Enami, 1983; Higashino, 1990). These are chlorite (300–360 °C, 5.5–6.5 kbar), garnet (425–470 °C, 7–8.5 kbar), albite–biotite (470–590 °C, 8–9.5 kbar) and oligoclase–biotite (585–635 °C, 9–11 kbar) zones (Fig. 1; Enami, 1983; Enami *et al.*, 1994). The mineral parageneses of the albite–biotite and oligo-

clase–biotite zones roughly coincide with those of epidote–amphibolite facies conditions, and their equilibrium P – T conditions have been estimated to be 8–11 kbar and 470–635 °C (Enami *et al.* 1994).

Eclogite facies assemblages sporadically occur in metabasite, metabasite, peridotite and minor amounts of metapelite in the epidote–amphibolite facies areas of the Besshi district in central Shikoku (e.g. Takasu 1989; Aoya 2001; Ota *et al.* 2004; Zaw Win Ko *et al.*, 2005; Kouketsu *et al.*, 2010; Kabir and Takasu, 2010a, b). These assemblages are considered to be evidence that the Sambagawa metamorphic rocks have partly experienced eclogite facies metamorphism before recrystallization under epidote–amphibolite facies conditions.

The Sebadani area belongs to the albite–biotite zone and is located in the central part of the Besshi district. The Sebadani area is mainly composed of the Seba basic schists with intercalation of pelitic and siliceous schists. Eclogites (Seba eclogitic basic schists) are sporadically preserved in the Seba basic

schists (Aoya, 2001; Zaw Win Ko *et al.*, 2005; Kabir and Takasu, 2009, 2010a, b), and they experienced three distinct events of metamorphism (Kabir and Takasu, 2009). These are a precursor metamorphic event (amphibolite facies), a first high-pressure metamorphic event (eclogite facies) and a second high-pressure metamorphic event (epidote–amphibolite facies). Since such complex metamorphic history of the Seba eclogitic basic schists, and clinopyroxene in the schists have various modes of occurrence and the variety of their chemical compositions.

In this paper we describe the variety of texture and chemical compositions of the clinopyroxenes from the Seba

eclogitic basic schists. Clinopyroxene end-member components were calculated on the basis of jadeite ($\text{NaAlSi}_2\text{O}_6$) (X_{Jd}) = lower value among Al^{VI} and Na in M_2 site, aegirine ($\text{NaFe}^{3+}\text{Si}_2\text{O}_6$) (X_{Aeg}) = lower value of Fe^{3+} in M_1 site among rest of Na in M_2 site and Quad (Ca-Mg-Fe pyroxene) = $1 - (\text{Jd} + \text{Aeg})$, wollastonite ($\text{Ca}_2\text{Si}_2\text{O}_6$) (X_{Wo}) = $\text{Ca}/(\text{Ca} + \text{Mg} + \Sigma\text{Fe})$ where $\Sigma\text{Fe} = (\text{Fe}^{2+} + \text{Fe}^{3+} + \text{Mn})$, enstatite ($\text{Mg}_2\text{Si}_2\text{O}_6$) (X_{En}) = $\text{Mg}/(\text{Ca} + \text{Mg} + \Sigma\text{Fe})$ and ferrosilite ($\text{Fe}^{2+}\text{Si}_2\text{O}_6$) (X_{Fs}) = $\Sigma\text{Fe}/(\text{Ca} + \text{Mg} + \Sigma\text{Fe})$ (Morimoto, 1989). The mineral abbreviations used in the text, tables and figures follow Whitney and Evans (2010), except for Agt, aegirine-augite.

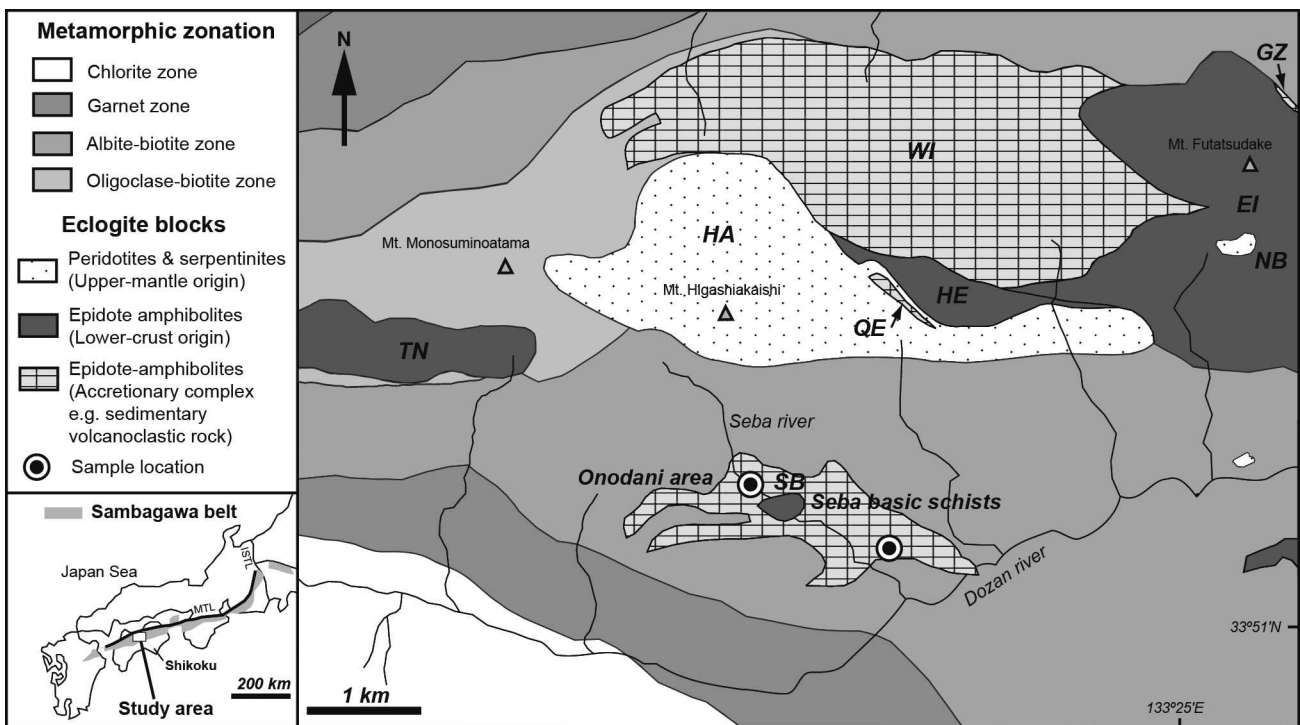


Figure 1. Geological and metamorphic zonal map of the Sambagawa metamorphic belt in the Besshi district, central Shikoku, Japan (compiled from Takasu and Makino, 1980; Takasu, 1989; Higashino, 1990; Kugimiya and Takasu, 2002; Sakurai and Takasu, 2009). SB, Sebadani metagabbro mass; TN, Tonaru metagabbro mass; WI, Western Iratsu mass; EI, Eastern Iratsu mass; HA, Higashi-akaishi peridotite mass; QE, Quartz eclogite mass; HE, Hornblende eclogite mass; NB, Nikubuchi peridotite mass; GZ, Gazo eclogite mass.

2. Petrography and the modes of occurrence of clinopyroxenes

The Seba eclogitic basic schists consist mainly of garnet, clinopyroxene (omphacite/aegirine-augite/augite), sodic/sodic-calcic/calcic-amphiboles (glaucofane, winchite, barroisite, Fe-barroisite, taramite, katophorite, Mg-katophorite, edenite, actinolite and Mg-hornblende), epidote and phengite (Fig. 2a-b). Minor amounts of rutile, titanite, albite, hematite and

quartz are also present. Chlorite, paragonite and carbonates (calcite and ankerite) occur occasionally. A schistosity is defined by preferred orientation of phengite, and a lineation is defined by aligned prismatic omphacite and sodic-calcic/calcic-amphibole (Kabir and Takasu, 2010b). Layers (< 4 mm) of carbonate minerals (calcite and ankerite) and large calcite patch (< 4 mm across) occur in the matrix.

Garnets occur as euhedral to subhedral porphyroblasts up to 5 mm in diameter. Some of them are optically zoned wi-

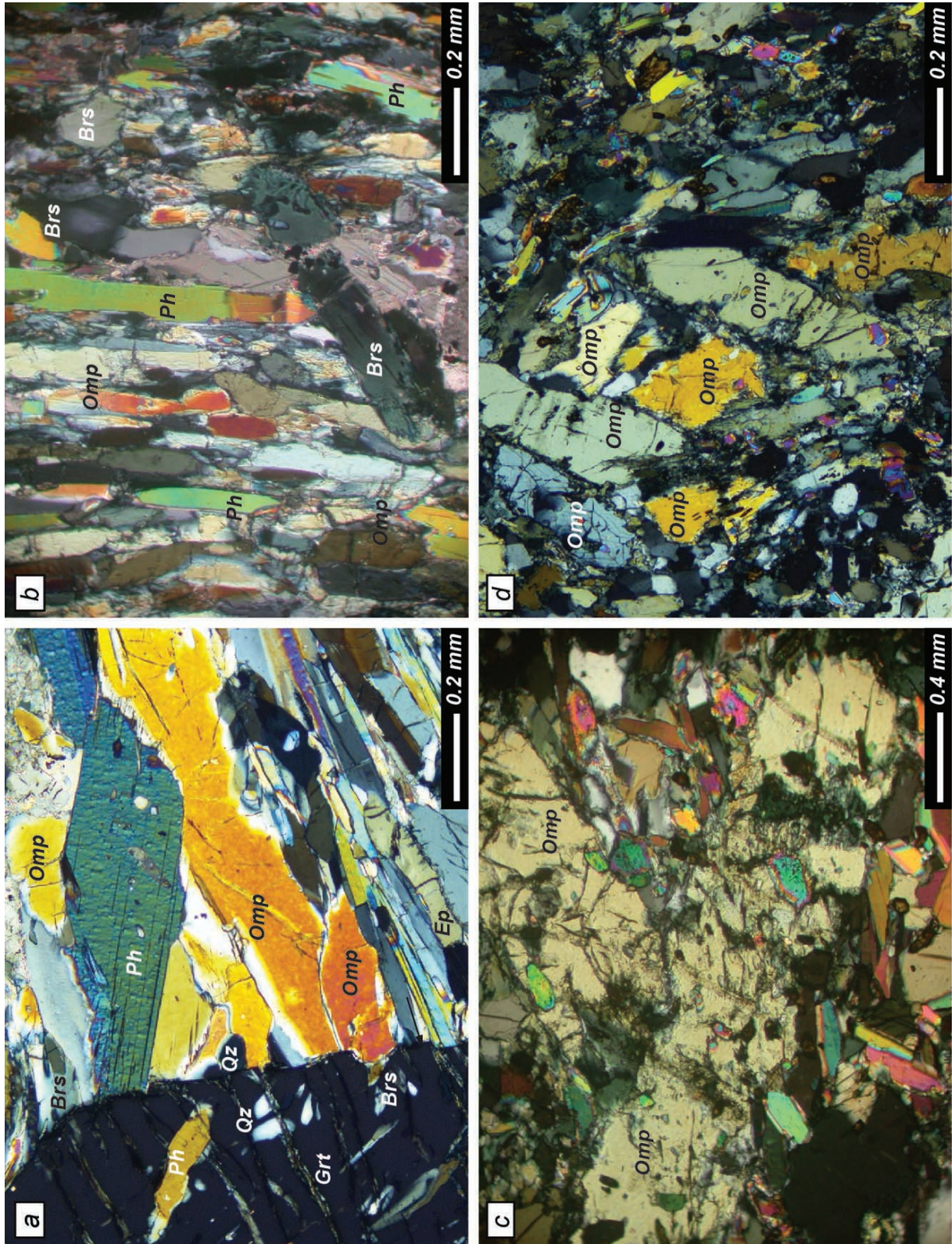


Figure 2. Photomicrographs of eclogite from the Seba eclogitic basic schists showing, (a) porphyroblastic garnet and schistosity-forming omphacite (Cpx-3), barroisite amphibole, phengite, epidote and quartz. The garnet contains inclusions of barroisite amphibole, phengite and quartz. (b) Schistosity-forming matrix omphacite (Cpx-3) and other matrix minerals (phengite, barroisite). (c-d) randomly oriented omphacites (Cpx-4) are cross-cutting to the matrix schistosity.

th pale orange-colored cores and colorless mantles. Both cores and mantles contain numerous inclusions and they commonly show a sigmoidal pattern. The cores of the garnets contain inclusions of sodic- and sodic-calcic amphiboles (glaucophane, winchite, barroisite), epidote ($X_{Ps} = 0.24\text{--}0.29$), paragonite, albite ($An < 3$), titanite, hematite, chlorite, calcite and quartz. The mantles of the garnets contain inclusions of clinopyroxene, sodic-calcic amphiboles (barroisite, taramite, katophorite), epidote ($X_{Ps} = 0.24\text{--}0.32$), phengite (Si = 6.65–6.81 cations per formula unit, pfu), rutile, titanite, albite ($An < 3$), chlorite and quartz (Kabir and Takasu, 2010b).

The clinopyroxenes in the Seba eclogitic basic schists commonly display five different mode of occurrence. Cpx-1 ($X_{Jd} = 0.23\text{--}0.39$) occurring as inclusions in the mantles of porphyroblastic garnets is euhedral to subhedral grains up to 1 mm across (Fig. 3a). Cpx-1 also occurs as a constituent mineral of polyphase inclusions, which consist of Cpx-1 (omphacite), amphibole (barroisite, Fe-barroisite, taramite) and phengite (Si = 6.65–6.69 pfu), and Cpx-1 (omphacite), amphibole (barroisite), epidote and phengite (Si = 6.70–6.74 pfu). Cpx-2 is documented as inclusions in coarse-grained epidotes and it occurs as subhedral fine grained relict crystals up to 0.03 mm across (Fig. 3b). Schistosity forming Cpx-3 occurring in the matrix forms subhedral prismatic grains up to 4 mm long (Fig. 2a-b). It is sometimes zoned with pale green cores to colorless rims. Cpx-3 contain inclusions of sodic-calcic amphiboles (barroisite), garnet, epidote, phengite (Si = 6.56–6.59 pfu), rutile, chlorite and calcite. Some clinopyroxenes are randomly oriented to the matrix schistosity (Cpx-4) (Fig. 2c-d) up to 4 mm long. They are sometimes zoned with pale green cores to colorless rims and contain inclusions of garnet, sodic-calcic amphiboles (barroisite, Mg-katophorite), epidote and rutile. Cpx-4 is partly replaced by symplectites of clinopyroxene (Cpx-5); augite, sodic-calcic/calcic-amphiboles (e.g. barroisite, edenite, actinolite), albite ($An < 4$) (Fig. 3c), and aegirine-augite, sodic-calcic/calcic-amphiboles (e.g. barroisite, edenite, Mg-hornblende) and albite ($An < 3$) (Fig. 3d).

3. Chemical compositions of clinopyroxenes

Chemical compositions and compositional zoning of the clinopyroxenes in the Seba eclogitic basic schists have been investigated by electron microprobe analyzer (JEOL JXA 8800M and 8530F) in Shimane University. Analytical conditions were 15 kV accelerating voltage, 20 nA specimen current

and 5 mm beam diameter for quantitative analysis. The correction was carried out by the procedure of Bence and Albee (1968). Fe^{3+} estimation for clinopyroxene used the $Fe^{3+} = 4 - 2 \times Si - 2 \times Ti - Al + Na$ (for 6 oxygen's). Ti (< 0.18 wt%), K (< 0.07 wt%) and Cr (< 0.08 wt%) are negligible for all clinopyroxenes.

Clinopyroxenes (Cpx-1) as inclusions in porphyroblastic garnets are classified as omphacite and aegirine-augite with $X_{Jd} = 0.23\text{--}0.39$ and $X_{Aeg} = 0\text{--}0.29$ (Fig. 4a; Table 1). Omphacite inclusions (Cpx-2) in coarse-grained epidotes have similar X_{Jd} (0.29–0.37) and X_{Aeg} (0.08–0.15) contents (Fig. 4a). Omphacites with preferred orientation in the matrix (Cpx-3) have relatively higher X_{Jd} ($X_{Jd} = 0.24\text{--}0.48$, $X_{Aeg} = 0\text{--}0.25$) contents than those included in garnets (Cpx-1) and epidotes (Cpx-2) (Fig. 4b).

The clinopyroxenes (Cpx-3) are occasionally zoned, with X_{Jd} increasing from core ($X_{Jd} = 0.25\text{--}0.36$, $X_{Aeg} = 0.05\text{--}0.17$) to rim ($X_{Jd} = 0.34\text{--}0.48$, $X_{Aeg} = 0.02\text{--}0.14$). Randomly oriented omphacites (Cpx-4) with $X_{Jd} = 0.25\text{--}0.36$ and $X_{Ac} = 0.10\text{--}0.24$ are slightly lower X_{Jd} contents than omphacites (Cpx-3) in the matrix (Fig. 4c). They are occasionally zoned with increasing X_{Jd} from core ($X_{Jd} = 0.27$, $X_{Aeg} = 0.20$) to rim ($X_{Jd} = 0.36$, $X_{Aeg} = 0.11$). Clinopyroxene (Cpx-5) as a constituent of the symplectite with sodic-calcic/calcic-amphiboles (e.g. barroisite, edenite, Mg-hornblende) and albite ($An < 3$) is aegirine-augite in composition and it has lower in $X_{Jd} = 0.11\text{--}0.19$ and higher in $X_{Aeg} = 0.32\text{--}0.36$ contents. Clinopyroxenes (Cpx-5) as a constituent of symplectite with sodic-calcic/calcic-amphiboles (e.g. barroisite, edenite, actinolite), albite ($An < 4$) is classified as augite (Ca-Fe-Mg pyroxenes) has lower in $X_{Jd} = 0.10\text{--}0.13$ and $X_{Aeg} = 0.01\text{--}0.07$ than all other modes of occurrences (Fig. 4b, d; Table 1). This clinopyroxene has quadrilateral compositions of $X_{Wo} = 0.21\text{--}0.23$, $X_{Fs} = 0.22\text{--}0.25$ and $X_{En} = 0.53\text{--}0.56$ contents (Fig. 4d).

4. Discussion and conclusions

The clinopyroxenes from the Seba eclogitic basic schists occur in various modes of occurrences. Their chemical compositions show a wide range of X_{Jd} from 0.10 to 0.48 including omphacite, aegirine-augite and augite compositions, responsible for a diversity of their equilibrium P – T conditions.

Aegirine-augite and omphacites (Cpx-1) inclusions in porphyroblastic garnets are crystallized before or during garnet growth. These clinopyroxenes are the products of the prograde

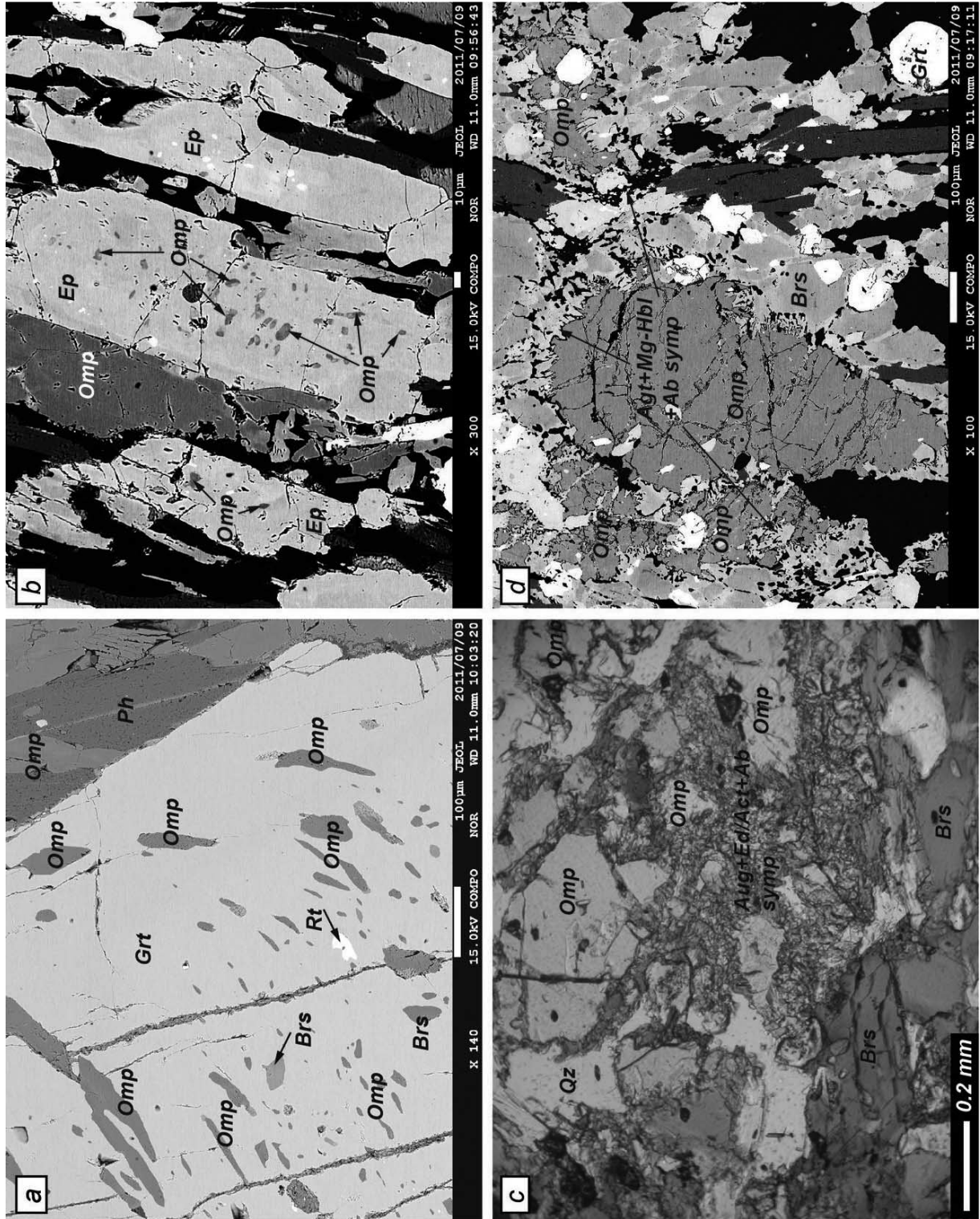


Figure 3. Backscattered electron images and photomicrograph of eclogites from the Seba eclogitic basic schists. (a) The garnet contains inclusions of omphacite (Cpx-1), barroisitic amphibole and rutile. (b) Large grains of matrix epidotes are coexisting with matrix omphacites (Cpx-3) containing inclusions of omphacite (Cpx-2). (c) Omphacites (Cpx-3) are replaced by symplectites of low-jadeite clinopyroxene (augite) (Cpx-5), edinitic/actinolitic amphibole and albite (An < 4) and (d) Actinolite-augite (Cpx-5), Mg-hornblende and albite (An < 3).

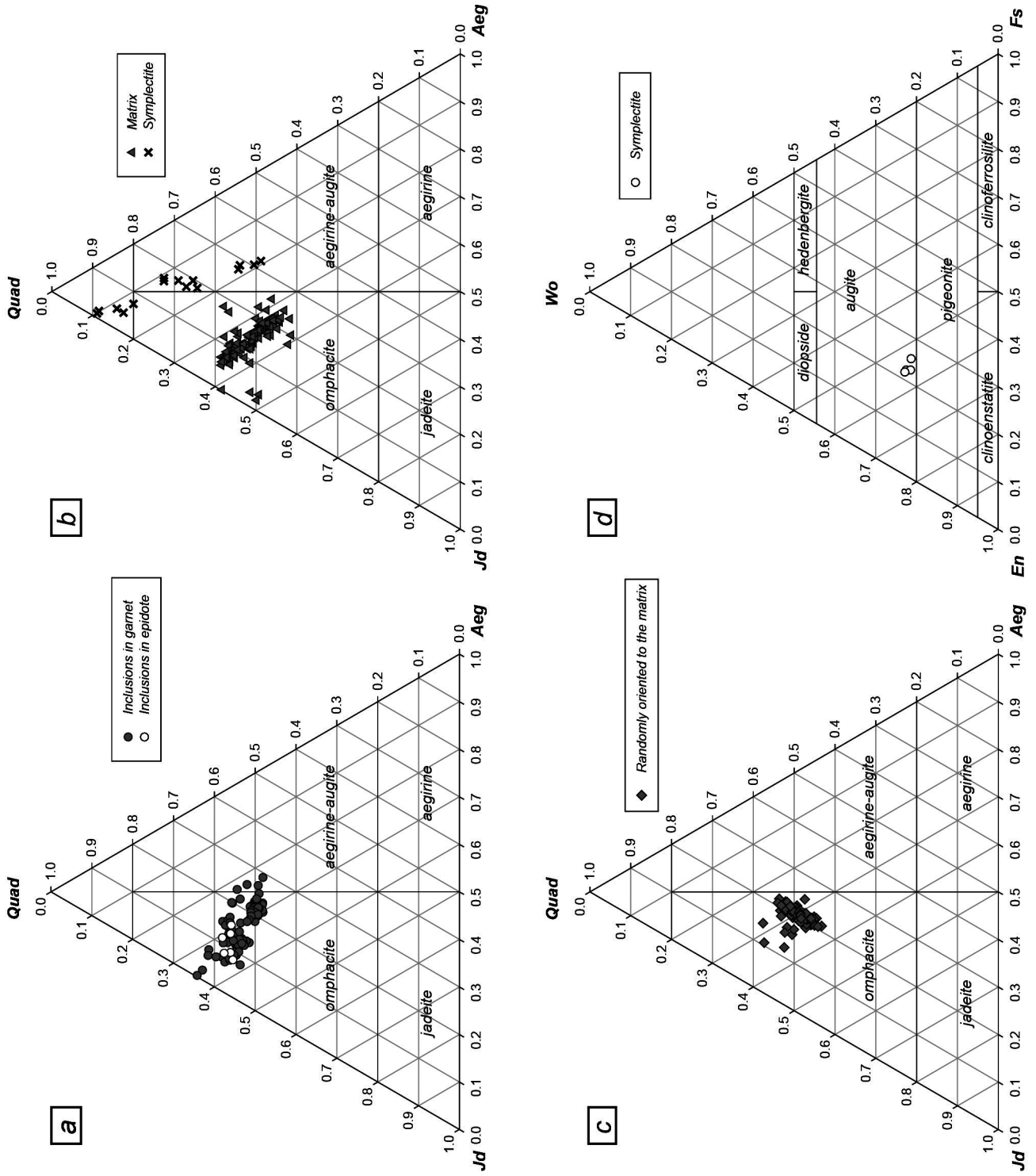


Figure 4. Variety of chemical compositions of clinopyroxenes from the Seba eclogitic basic schists (after Morimoto, 1989).

to the peak metamorphism of epidote–amphibolite and eclogite facies metamorphic conditions. X_{Jd} of Cpx-1 included in the mantle of the garnets increases from Cpx-1 included in the inner mantle to that included in the outermost mantle, ranging from 0.23 to 0.39. The Fe^{2+} –Mg partitioning between garnet and omphacite inclusion (K_D) ranges between 11 and 23, and X_{Jd} of the omphacite range from 0.23 to 0.39. The P – T conditions were estimated from the calibrations of the garnet–clinopyroxene Fe^{2+} –Mg exchange geothermometry, giving from 535 °C to 680 °C (Ellis and Green, 1979) from inner

mantle pairs to the outermost mantle pairs. These suggest that metamorphic temperatures increase during the growth of garnets (Fig. 5). The clinopyroxene inclusions in the outermost mantle and their host garnets are crystallized close to the peak metamorphic conditions of the eclogite facies. Clinopyroxenes as inclusions in the large epidotes (Cpx-2) probably crystallized simultaneously with Cpx-1 during the prograde metamorphism, because matrix omphacites and epidotes are coexisted and the X_{Jd} of Cpx-1 and Cpx-2 are the similar.

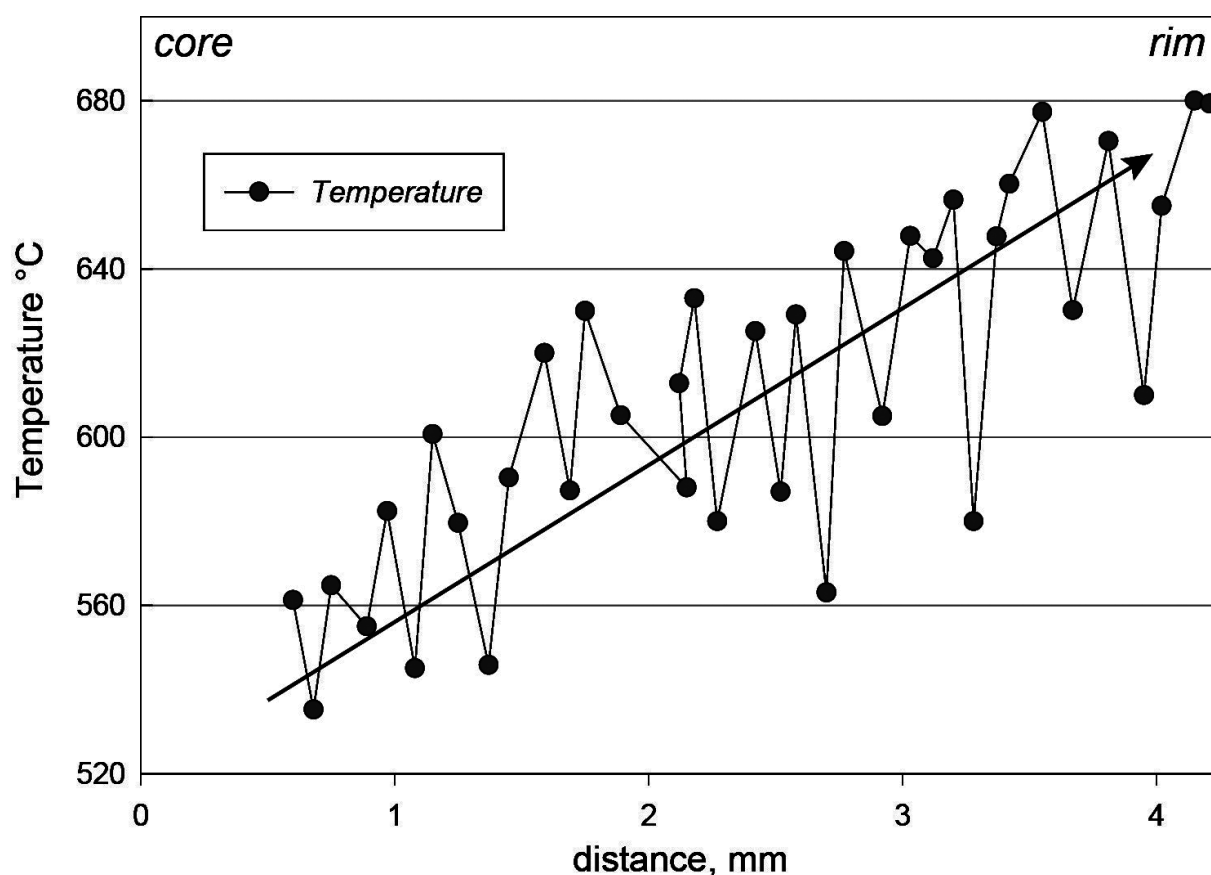


Figure 5. Estimated metamorphic temperature using Fe^{2+}/Mg exchange reaction between inclusions omphacite versus host garnet (Ellis and Green, 1979) represents metamorphic temperature increase from garnet core to the rim (solid arrow).

The peak metamorphic conditions of eclogite facies are defined by the schistosity forming minerals coexisting with the outermost mantle of porphyroblastic garnet, omphacite (Cpx-3), barroisitic amphibole, phengite ($Si = 6.62$ – 6.88 pfu), rutile and quartz (Kabir and Takasu, 2010b). The estimated peak metamorphic conditions of the eclogites are 12–24 kbar and 610–640 °C (Aoya, 2001; Kabir and Takasu, 2010c). Cpx-4 occurring as randomly oriented to the matrix foliation is similar to those of omphacites in R-type eclogites (Aoya and Wal-

lis, 1999). Aoya and Wallis (1999) reported R-type eclogite have been found only in the area adjacent to the Sebadani metagabbro mass, while R-type eclogites were also reported 1 km away from the mass (Kabir and Takasu, 2010c). The eclogites in the Seba eclogitic basic schists were affected by deformation of varying degrees resulting in the formation of a variety of textural types of omphacites (e.g. lineated and randomly oriented) (Aoya and Wallis, 1999). The retrograde stage is defined by the phases replacing the minerals of the peak metamorphic

stage. The omphacites are replaced by symplectites of aegirine-augite ($X_{\text{Jd}} = 0.11\text{--}0.19$), sodic-calcic/calcic-amphiboles (e.g. barroisite, edenite, Mg-hornblende) and albite ($An < 3$) or symplectite of augite ($X_{\text{Jd}} = 0.10\text{--}0.13$), sodic-calcic/calcic-amphiboles (e.g. barroisite, edenite, actinolite) and albite ($An < 4$). Temperature of 420–490 °C and pressure of 6–7 kbar at the epidote-amphibolite facies conditions are obtained from the Cpx-5 ($X_{\text{Jd}} = 0.10\text{--}0.19$), sodic-calcic/calcic-amphiboles and albite by THERMOCALC (Holland and Powell, 1998) (Kabir and Takasu, 2010b).

Acknowledgements

We thank the members of the Geoscience seminar and the Metamorphic Geology seminar of Shimane University for discussion and helpful suggestions.

References

- Aoya, M. and Wallis, S. R., 1999, Structural and microstructural constraints on the mechanism of eclogite formation in the Sambagawa belt, SW Japan. *Journal of Structural Geology*, 21, 1561–1573.
- Aoya, M., 2001, P – T – D path of eclogite from the Sambagawa belt deduced from combination of petrological and microstructural analysis. *Journal of Petrology*, 42 (7), 1225–1248.
- Banno, S., 1964, Petrological studies of the Sanbagawa crystalline schists in the Bessi-Ino district, central Shikoku, Japan. *Journal of the Faculty of Science, Tokyo University, Section II*, 15, 203–319.
- Bence, A. E. and Albee, A. L., 1968, Empirical correction factors for the electron microanalysis of silicates and oxides. *Journal of Geology*, 76, 382–403.
- Ellis, D. J. and Green, D. H., 1979, An experimental study of the effect of Ca upon garnet-clinopyroxene Fe–Mg exchange equilibria. *Contributions to Mineralogy and Petrology*, 71, 13–22.
- Enami, M., 1983, Petrology of pelitic schists in the oligoclase-biotite zone of the Sanbagawa metamorphic terrain, Japan: Phase equilibria in the highest grade zone of a high-pressure intermediate type of metamorphic belt. *Journal of Metamorphic Geology*, 1, 141–161.
- Enami, M., Wallis, S. R. and Banno, Y., 1994, Paragenesis of sodic pyroxene-bearing quartz schist: implications for the P – T history of the Sanbagawa belt. *Contributions to Mineralogy and Petrology*, 116, 182–198.
- Higashino, T., 1990, The higher grade metamorphic zonation of the Sambagawa metamorphic belt in central Shikoku, Japan. *Journal of Metamorphic Geology*, 8, 413–423.
- Holland, T. J. B. and Powell, R., 1998, An internally consistent thermodynamic data set for phases of petrological interest. *Journal of Metamorphic Geology*, 16, 309–343.
- Kabir, M. F. and Takasu, A., 2009, Polyphase metamorphic history of pelitic schists in the Sambagawa metamorphic belt, Sebadani area, central Shikoku, Japan. *Annual Meeting, Geological Society of Japan*, Okayama University of Science, Okayama, Japan, p. 148.
- Kabir, M. F. and Takasu, A., 2010a, Evidence for multiple burial–partial exhumation cycles from the Onodani eclogites in the Sambagawa metamorphic belt, central Shikoku, Japan. *Journal of Metamorphic Geology*, 28, 873–893.
- Kabir, M. F. and Takasu, A., 2010b, Glaucophanic amphibole in the Seba eclogitic basic schists, Sambagawa metamorphic belt, central Shikoku, Japan: implications for timing of juxtaposition of the eclogite body with the non-eclogite Sambagawa schists. *Earth Science*, 64, 183–192.
- Kabir, M. F. and Takasu, A., 2010c, Polyphase high-pressure metamorphism of the Sebadani–Onodani eclogites in the Sambagawa metamorphic belt, central Shikoku, Japan: evidence for multiple burial and exhumation cycles of eclogites. *Abstract of Annual Meeting, Japan Association of Mineralogical Sciences*, Shimane University, Japan, p. 205.
- Kouketsu, Y., Enami, M. and Mizukami, T., 2010, Omphacite-bearing metapelite from the Besshi region, Sambagawa metamorphic belt, Japan: Prograde eclogite facies metamorphism recorded in metasediment. *Journal of Mineralogical and Petrological Sciences*, 105, 9–19.
- Kugimiya, Y. and Takasu, A., 2002, Geology of the Western Iratsu mass within the tectonic mélange zone in the Sambagawa Metamorphic Belt, Besshi district, central Shikoku, Japan. *Journal of the Geological Society of Japan*, 108, 644–662 (in Japanese with English abstract).
- Morimoto, N., 1989, Nomenclature of pyroxenes. *Canadian Mineralogist*, 27, 143–156.
- Ota, T., Terabayashi, M. and Katayama, I., 2004, Thermobaric structure and metamorphic evolution of the eclogite body in the Sanbagawa belt, central Shikoku, Japan. *Lithos*, 73,

95–126.

- Sakurai, T. and Takasu, A., 2009, Geology and metamorphism of the Gazo mass (eclogite-bearing tectonic block) in the Sambagawa metamorphic belt, Besshi district, central Shikoku, Japan. *Journal of the Geological Society of Japan*, 115, 101–121 (in Japanese with English abstract).
- Takasu, A. and Makino, K., 1980, Stratigraphy and geologic structure of the Sanbagawa metamorphic belt in the Besshi district, Shikoku, Japan (Reexamination of the recumbent fold structures). *Earth Science*, 34, 16–26 (in Japanese with English abstract).
- Takasu, A., 1989, *P–T* histories of peridotite and amphibolite tectonic blocks in the Sanbagawa metamorphic belt, Japan. In: *Evolution of metamorphic belts*, Special Publication, (eds Daly, J.S., Cliff, R.A. and Yardley, B.W.D.), 43, 533–538. Geological Society, London.
- Whitney, D. L. and Evans, B. W., 2010. Abbreviations for names of rock-forming minerals. *American Mineralogist*, 95, 185–187.
- Zaw Win Ko, Enami, M. and Aoya, M., 2005, Chloritoid and barroisite-bearing pelitic schist from the eclogite unit in the Besshi district, Sanbagawa metamorphic belt. *Lithos*, 81, 79–100.

Table 1. (continued)

Sample	SEB-M-02																		
Analysis	46	47	49	51	53	56	58	61	65	66	69	70	73	77	80	82	3	4	6
	Cpx-1	Cpx-1	Cpx-1	Cpx-1	Cpx-1	Cpx-1	Cpx-1	Cpx-1	Cpx-1	Cpx-1	Cpx-3	Cpx-3	Cpx-3	Cpx-1	Cpx-1	Cpx-1	Cpx-2	Cpx-3	Cpx-2
SiO ₂	54.57	54.50	54.05	54.19	54.37	52.72	53.47	54.83	53.45	52.53	53.52	54.02	55.20	53.57	54.05	54.05	54.71	55.59	55.31
TiO ₂	0.02	0.07	0.03	0.05	0.04	0.04	0.05	0.09	0.07	0.01	0.11	0.03	0.02	0.05	0.00	0.06	0.05	0.05	0.13
Al ₂ O ₃	7.37	8.08	7.60	8.00	7.55	8.95	5.64	8.02	6.61	7.33	6.28	8.28	7.57	5.74	7.74	7.77	6.88	8.97	8.34
FeO*	10.10	11.09	10.60	10.61	11.21	11.81	13.00	11.14	12.03	12.14	12.48	11.25	10.54	13.94	10.70	11.34	10.45	7.65	8.32
MnO	0.05	0.05	0.11	0.04	0.03	0.09	0.02	0.09	0.03	0.12	0.05	0.10	0.09	0.05	0.01	0.07	0.08	0.04	0.00
MgO	7.42	6.89	7.36	7.14	7.06	6.66	7.17	7.16	7.60	7.23	6.96	7.06	7.64	6.96	7.29	7.04	7.66	7.55	8.12
CaO	13.49	12.54	13.33	13.17	13.26	12.08	13.36	12.75	13.55	13.13	13.01	12.87	13.42	12.66	13.16	13.03	14.20	14.00	14.53
Na ₂ O	6.32	6.80	6.31	6.51	6.11	6.49	6.16	6.74	6.00	5.86	6.08	6.39	6.58	6.49	6.50	6.54	6.29	6.83	6.36
K ₂ O	0.02	0.01	0.03	0.06	0.04	0.02	0.03	0.04	0.03	0.04	0.01	0.03	0.04	0.04	0.05	0.04	0.07	0.02	0.04
Cr ₂ O ₃	0.00	0.02	0.00	0.00	0.00	0.00	0.03	0.01	0.01	0.03	0.01	0.01	0.00	0.00	0.02	0.04	0.00	0.00	0.00
Total	99.37	100.05	99.42	99.76	99.66	98.86	98.93	100.86	99.37	98.43	98.51	100.04	101.11	99.50	99.51	99.97	100.39	100.71	101.15
<i>Cations on the basis of 6 oxygens</i>																			
Si	2.017	2.006	2.003	1.999	2.011	1.971	2.019	2.003	1.999	1.984	2.020	1.991	2.009	2.017	2.001	1.998	2.011	2.004	1.995
Ti	0.001	0.002	0.001	0.001	0.001	0.001	0.002	0.002	0.002	0.000	0.003	0.001	0.001	0.001	0.000	0.002	0.001	0.001	0.004
Al	0.321	0.350	0.332	0.348	0.329	0.394	0.251	0.345	0.291	0.326	0.279	0.360	0.325	0.255	0.338	0.339	0.298	0.381	0.354
Fe*	0.312	0.341	0.328	0.327	0.347	0.369	0.411	0.340	0.376	0.383	0.394	0.347	0.321	0.439	0.331	0.351	0.321	0.231	0.251
Mn	0.002	0.002	0.003	0.001	0.001	0.003	0.001	0.003	0.001	0.004	0.002	0.003	0.003	0.002	0.000	0.002	0.002	0.001	0.000
Mg	0.409	0.378	0.407	0.393	0.389	0.371	0.404	0.390	0.424	0.407	0.392	0.388	0.415	0.391	0.403	0.388	0.419	0.406	0.437
Ca	0.534	0.494	0.529	0.521	0.525	0.484	0.540	0.499	0.543	0.531	0.526	0.508	0.523	0.511	0.522	0.516	0.559	0.541	0.561
Na	0.453	0.485	0.454	0.465	0.438	0.471	0.451	0.477	0.435	0.429	0.445	0.457	0.464	0.474	0.467	0.469	0.448	0.478	0.445
K	0.001	0.001	0.001	0.003	0.002	0.001	0.001	0.002	0.001	0.002	0.000	0.001	0.002	0.002	0.002	0.002	0.003	0.001	0.002
Cr	0.000	0.001	0.000	0.000	0.000	0.000	0.001	0.000	0.000	0.001	0.000	0.000	0.000	0.000	0.001	0.001	0.000	0.000	0.000
Total	4.049	4.060	4.058	4.059	4.043	4.066	4.080	4.062	4.072	4.068	4.060	4.057	4.062	4.092	4.064	4.066	4.065	4.043	4.048
Sample	SEB-M-02																		
Analysis	15	16	25	34	138	28	29	30	36	42	45	61	62	16	34	25	138	139	
	Cpx-2	Cpx-2	Cpx-1	Cpx-1	Cpx-1	Cpx-1	Cpx-1	Cpx-1	Cpx-1	Cpx-1	Cpx-1	Cpx-1	Cpx-1	Cpx-3	Cpx-3	Cpx-3	Cpx-3	Cpx-3	
SiO ₂	55.32	55.24	54.80	55.72	55.21	54.60	54.97	54.52	55.39	55.22	55.66	55.34	54.82	54.24	55.72	54.80	55.21	54.03	
TiO ₂	0.14	0.07	0.06	0.05	0.05	0.10	0.03	0.07	0.03	0.06	0.03	0.09	0.06	0.07	0.05	0.06	0.05	0.03	
Al ₂ O ₃	8.17	5.75	10.91	11.20	11.40	8.26	8.37	6.77	7.29	7.80	8.26	8.61	7.54	5.75	11.20	10.91	11.40	7.20	
FeO*	8.75	10.84	7.87	6.84	6.32	11.16	10.03	11.51	9.92	10.33	8.93	8.33	9.75	10.84	6.84	7.87	6.32	8.59	
MnO	0.03	0.42	0.58	0.32	0.21	0.03	0.09	0.04	0.04	0.07	0.10	0.01	0.06	0.42	0.32	0.58	0.21	0.15	
MgO	8.10	8.51	6.98	6.57	6.76	6.92	7.34	7.69	8.30	7.33	7.78	8.31	8.04	8.51	6.57	6.98	6.76	8.56	
CaO	14.65	14.97	12.68	11.86	12.42	13.23	13.60	14.41	15.05	14.35	14.02	14.52	14.21	14.97	11.86	12.68	12.42	14.53	
Na ₂ O	6.12	6.05	7.07	7.32	7.23	6.79	6.84	6.30	6.46	6.44	6.80	6.34	6.67	6.05	7.32	7.07	7.23	6.00	
K ₂ O	0.04	0.04	0.04	0.04	0.03	0.04	0.02	0.04	0.02	0.02	0.03	0.02	0.03	0.04	0.04	0.04	0.03	0.04	
Cr ₂ O ₃	0.00	0.00	0.01	0.01	0.03	0.01	0.03	0.00	0.00	0.04	0.04	0.02	0.00	0.00	0.01	0.01	0.03	0.00	
Total	101.33	100.89	100.98	99.92	99.64	101.12	101.32	101.35	102.50	101.66	101.66	101.60	101.16	100.89	99.92	100.98	99.64	99.13	
<i>Cations on the basis of 6 oxygens</i>																			
Si	1.995	1.999	1.970	2.003	1.989	1.993	1.994	1.997	1.992	2.000	2.002	1.986	1.994	1.999	2.003	1.970	1.989	1.997	
Ti	0.004	0.002	0.002	0.001	0.001	0.003	0.001	0.002	0.001	0.002	0.001	0.003	0.002	0.002	0.001	0.002	0.001	0.001	
Al	0.347	0.250	0.462	0.474	0.484	0.355	0.358	0.292	0.309	0.333	0.350	0.364	0.323	0.250	0.474	0.462	0.484	0.314	
Fe*	0.264	0.334	0.236	0.206	0.191	0.341	0.304	0.353	0.298	0.313	0.269	0.250	0.297	0.334	0.206	0.236	0.191	0.266	
Mn	0.001	0.013	0.018	0.010	0.006	0.001	0.003	0.001	0.001	0.002	0.003	0.000	0.002	0.013	0.010	0.018	0.006	0.005	
Mg	0.435	0.468	0.374	0.352	0.363	0.376	0.397	0.420	0.445	0.396	0.417	0.445	0.436	0.468	0.352	0.374	0.363	0.472	
Ca	0.566	0.591	0.488	0.457	0.479	0.517	0.528	0.565	0.580	0.557	0.540	0.558	0.554	0.591	0.457	0.488	0.479	0.576	
Na	0.428	0.432	0.492	0.510	0.505	0.481	0.481	0.447	0.450	0.452	0.474	0.441	0.470	0.432	0.510	0.492	0.505	0.430	
K	0.002	0.002	0.002	0.002	0.001	0.002	0.001	0.002	0.001	0.001	0.001	0.001	0.002	0.002	0.002	0.002	0.001	0.002	
Cr	0.000	0.000	0.000	0.000	0.001	0.000	0.001	0.000	0.000	0.001	0.001	0.001	0.000	0.000	0.000	0.000	0.001	0.000	
Total	4.043	4.091	4.044	4.015	4.020	4.068	4.067	4.079	4.078	4.058	4.059	4.050	4.079	4.091	4.015	4.044	4.020	4.061	

*Total Fe as FeO